Fracture of Anisotropic Rock

E. Hoek

South African Council for Scientific and Industrial Research

Journal of the South African Institute of Mining and Metallurgy
Volume 64, Pages 501-518, No. 10, May 1964

Introduction

Due to their disposition, most rocks of sedimentary origin which occur in the upper layers of the earth's crust exhibit some degree of anisotropy when subjected to stress. Since the deformation and fracture of these rocks is of importance to engineers concerned with the design of shallow mining excavations or of foundations for civil engineering structures, it is obvious that research into the effects of anisotropy on rock behaviour is necessary.

Most of the published research on anisotropic rock is of an experimental nature [1, 2, 3] and in this paper an attempt is made to formulate a theoretical explanation for the observed fracture behaviour. This theoretical approach is based upon Griffith's postulate that fracture initiates from exiting cracks and flaws inherent in any brittle material [4, 5, 6]. In the case of an anisotropic rock, these cracks are assumed to be oriented preferentially along bedding planes. The effect of anisotropy on the deformation and stress distribution prior to fracture is not considered in this paper.

Results of triaxial strength tests on a South African slate are in good agreement with the theoretical predictions.

Griffith's theory of brittle fracture

The currently accepted interpretation of Griffith's theory of brittle fracture [4, 5] is that fracture initiates when the molecular cohesive strength of the material is exceeded by the tensile stresses at the tips of inherent cracks and flaws in the material [6, 7]. If it is assumed that these cracks and flaws are elliptical in shape, then the results presented by Inglis [8] can be used to calculate the stresses induced around the boundary of these very flat elliptical cracks.

The stress system acting upon an elliptical crack is illustrated Figure 1. The ellipse and the surrounding stress field are related to the elliptical coordinates η and ε which are defined by the following equations of transformation of a rectangular system of coordinates x and z:

$$x = c \sinh \varepsilon \sin \eta,$$
$$z = c \cosh \varepsilon \cos \eta$$

The stress system acting on the crack is given by two normal components σ_{xx} and σ_{zz} and a shear component τ_{xz}. The stress σ_{zz}, which acts parallel to the major axis of the crack, has a negligible influence upon the stresses induced near the crack tip and need not be considered in the following analysis, The stresses σ_{xx} and τ_{xz} are related to the principal stresses σ_1 and σ_3 by the following equations:

$$2\sigma_{xx} = (\sigma_1 + \sigma_3) - (\sigma_1 - \sigma_3)\cos 2\psi \tag{1}$$
$$2\tau_{xz} = (\sigma_1 - \sigma_3)\sin 2\psi \tag{2}$$

Where ψ is the angle between the major axis of the elliptical crack and the direction of the major principal stress σ_1. Note that σ_1 is defined as the algebraically largest and σ_3 the algebraically smallest of the three principal stresses. The sign convention used in this paper is such that *compressive* stresses are taken as *positive.*

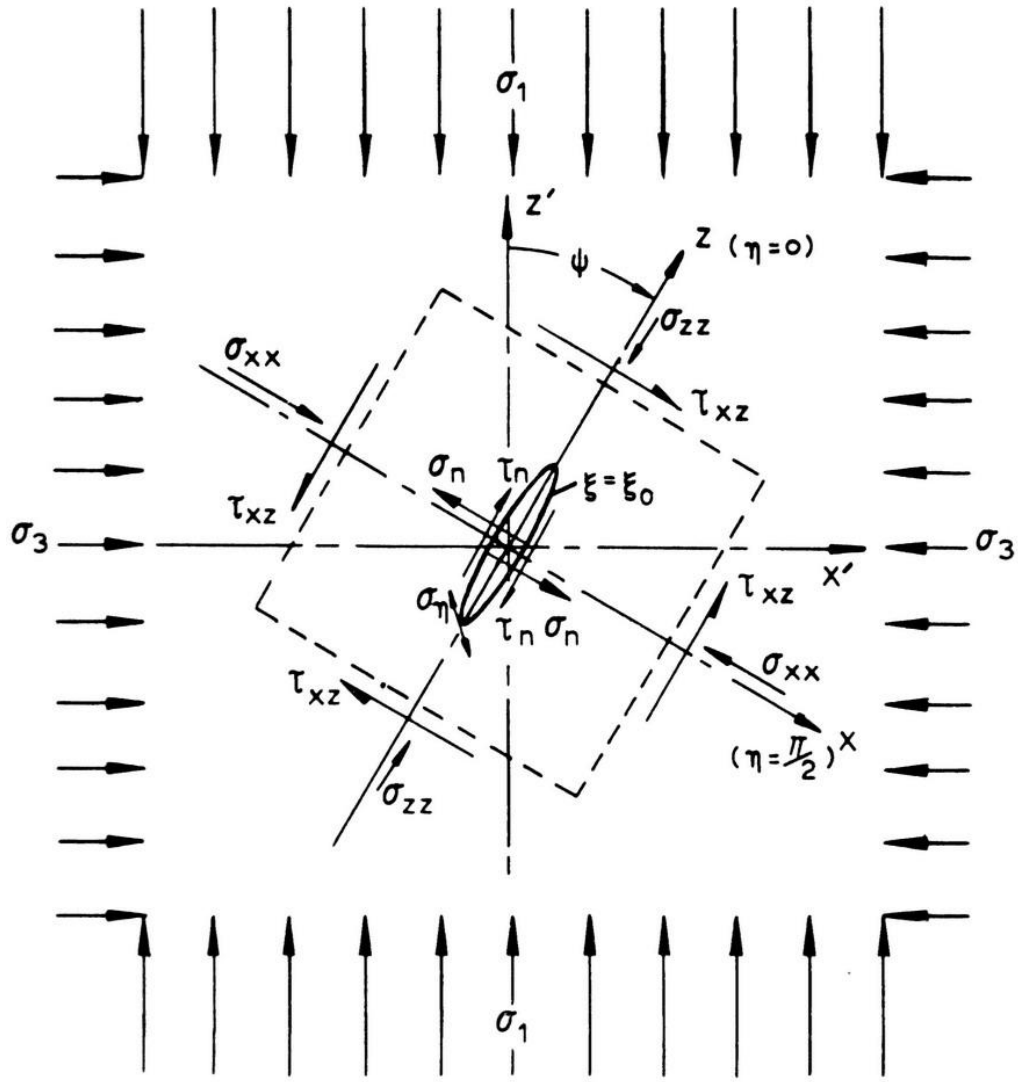

Figure 1. Stresses acting upon a crack which is inclined at an angle ψ to the direction of the major principal stress σ_1

The stresses σ_n and τ_n which act on the surface of the crack as shown in Figure 1 exist only when closure of the crack has occurred and their influence is considered in a later section of this paper which deals with the effects of crack closure.

The tangential stress σ_n at the boundary of an open elliptical crack, due to the applied stresses σ_{xx} and τ_{xx}, neglecting σ_{zz} is given by the following equation [8]:

$$\sigma_\eta = \frac{\sigma_{xx}\left(\sinh 2\xi_0 + e^2\xi_0 \cdot \cos 2\eta - 1\right) + 2\tau_{xz} \cdot e^2\xi_0 \cdot \sin 2\eta}{\cosh 2\xi_0 - \cos 2\eta} \tag{3}$$

Where ξ_0 is the value of the elliptical coordinate ξ on the crack boundary.

The maximum tangential stresses, both tensile and compressive, occur near the ends of the crack, i.e. when the value of η is small. Since the value of ξ_0 is also small for a very flat ellipse, equation (3) may be simplified by series expansion in which terms of the second order and higher which appear in the numerator are neglected. This simplification results in the following equation, valid only for the stresses near the crack tip:

$$\sigma_\eta = 2\left\{\frac{\sigma_{xx} \cdot \xi_0 + \tau_{xz} \cdot \eta}{\xi_0{}^2 + \eta^2}\right\} \tag{4}$$

Differentiation of equation (4) with respect to η and equating $\partial\sigma_\eta / \partial\eta$ to zero results in a quadratic equation in η from which the positions on the crack boundary at which the maximum and minimum stresses occur can be determined. Substituting these values of η into equation (4) gives the maximum and minimum stresses on the crack boundary as

$$\sigma_N \cdot \xi_0 = \sigma_{xx} \pm \sqrt{\sigma_{xx}^2 + \tau_{xz}^2} \tag{5}$$

Where σ_N is the maximum value of σ_η .

Expressing equation (5) in terms of the principal stresses σ_1 and σ_3 from equations (1) and (2) gives

$$\sigma_N \cdot \xi_0 = \frac{1}{2}\left[(\sigma_1 + \sigma_3) - (\sigma_1 - \sigma_3)\cos 2\psi\right] \pm \sqrt{\frac{1}{2}\left[\left(\sigma_1^2 + \sigma_3^2\right) - \left(\sigma_1^2 - \sigma_3^2\right)\cos 2\psi\right]} \tag{6}$$

The critical crack orientation ψ_c at which the maximum and minimum stresses are induced at or near the crack tip is found by differentiating equation (6) with respect to ψ and letting $\partial\sigma_\eta / \partial\psi = 0$. This gives

$$Cos\,2\psi_c = \frac{\sigma_1 - \sigma_3}{2(\sigma_1 + \sigma_3)} = \frac{1-k}{2(1+k)} \tag{7}$$

Where $k = \sigma_3/\sigma_1$.

Note that equation (7) is only meaningful if $k \geq -0.33$. When $k = -0.33$ then $\cos 2\psi_c = 1$. Substituting this value into equation (6) gives

$$\sigma_c \cdot \xi_0 = 2\sigma_3 \tag{8}$$

Where σ_c is the maximum value of the tangential stress σ_η at the critical crack orientation ψ_c.

In other words, for $k \leq -0.33$ the maximum tensile stress at the crack tip depends upon the magnitude of the minor principal stress σ_3 only and, since this stress is tensile because k is negative, fracture occurs when the minor principal stress attains the uniaxial tensile strength of the material. Since the strength of a material cannot be lower than its uniaxial tensile strength, the fracture condition expressed in equation (8) holds for the entire range $-\infty < k \leq -0.33$. The critical crack orientation ψ_c remains unchanged at zero $(\cos 2\psi_c = 1)$.

Denoting the uniaxial tensile strength of the material by σ_t, equation (8) can be re-written as

$$\sigma_c \cdot \xi_0 = 2\sigma_t \tag{9}$$

The term $\sigma_c \cdot \xi_0$ which appears in equations (8) and (9) is a product of the cohesive strength σ_c of the material and the parameter ξ_0 which defines the shape of the crack. Both of these parameters are difficult to evaluate under practical conditions but equation (9) offers the opportunity of determining their product fairly readily.

Substituting equation (9) into equation (6) gives the following relationship between the stresses required to initiate fracture from a crack inclined at the angle ψ to the direction of σ_1 and the uniaxial tensile strength of the material.

$$2\sigma_t = \frac{1}{2}\left[(\sigma_1 + \sigma_3) - (\sigma_1 - \sigma_3)\cos 2\psi\right] \pm \sqrt{\frac{1}{2}\left[\left(\sigma_1^2 + \sigma_3^2\right) - \left(\sigma_1^2 - \sigma_3^2\right)\cos 2\psi\right]} \tag{10}$$

In the case of a homogeneous, isotropic material, it is normally assumed that the inherent cracks are randomly distributed throughout the specimen and that fracture will initiate from those cracks which are inclined at the angle ψ_c defined by equation (7).

Substituting equation (7) into equation (10) results in the following fracture criterion for such a material:

$$\sigma_1 = \frac{-8\sigma_t\ (1+k)}{(1-k)^2} \tag{11}$$

In the case of an anisotropic material where the weakest cracks are assumed to lie in the bedding planes, it is necessary to consider the orientation of these cracks in relation to the applied stress system in order to determine the fracture conditions. In this case, the fracture criterion is expressed by equation (10) where ψ is the orientation of the weakest cracks to the direction of the major principal stress σ_1. A graphical representation of this equation is given in Figure 2.

Modified fracture criterion for closed cracks

In deriving the fracture criterion outlined above, it has been assumed that the shape of the crack does not change until fracture occurs. In other words, the elliptical crack remains open under all conditions of applied stress. While this may be true for predominantly tensile stress fields, it certainly does not hold for the case of very flat cracks which are subjected to compressive stress. Consequently, it is necessary to consider the effects of crack closure upon the Griffith's fracture criterion.

In the following analysis, based upon the modification to Griffith's theory by McClintock and Walsh [9], it is assumed that the initial crack in an unstressed body is uniformly closed over its entire length. If the normal stress σ_{xx} is tensile, the crack opens and the Griffith's criterion holds. If the normal stress σ_{xx} is compressive (positive) then a stress $\sigma_n = \sigma_{xx}$ results from the reaction between the crack surfaces. Under these conditions, the stress σ_{xx} is transmitted across the crack without influencing the stresses induced at the crack tips and, hence, it plays no direct part in the fracture process.

In addition, however, a frictional shear resistance τ_n occurs parallel to the crack as a result of the contact pressure between the crack surfaces. Denoting the coefficient of friction between these surfaces by μ;

$$\tau_n = \mu\sigma_n = \mu\sigma_{xx} \tag{12}$$

The shear stress τ_{xz} can only induce tensile stresses at the crack tip when this frictional resistance has been overcome and when relative movement between the crack surfaces can occur. Consequently, the net shear stress which is effective in inducing tensile stresses at the crack boundary is $\tau_{xz} - \tau_n$ or $\tau_{xz} - \mu\sigma_{xx}$.

From Equation (4), the tangential stress σ_η on the boundary of a closed crack due to the net shear stress $\tau_{xz} - \mu\sigma_{xx}$ is

$$\sigma_\eta = \frac{2\,\eta\,(\tau_{xz} - \mu\sigma_{xx})}{\xi_0^2 + \eta^2} \tag{13}$$

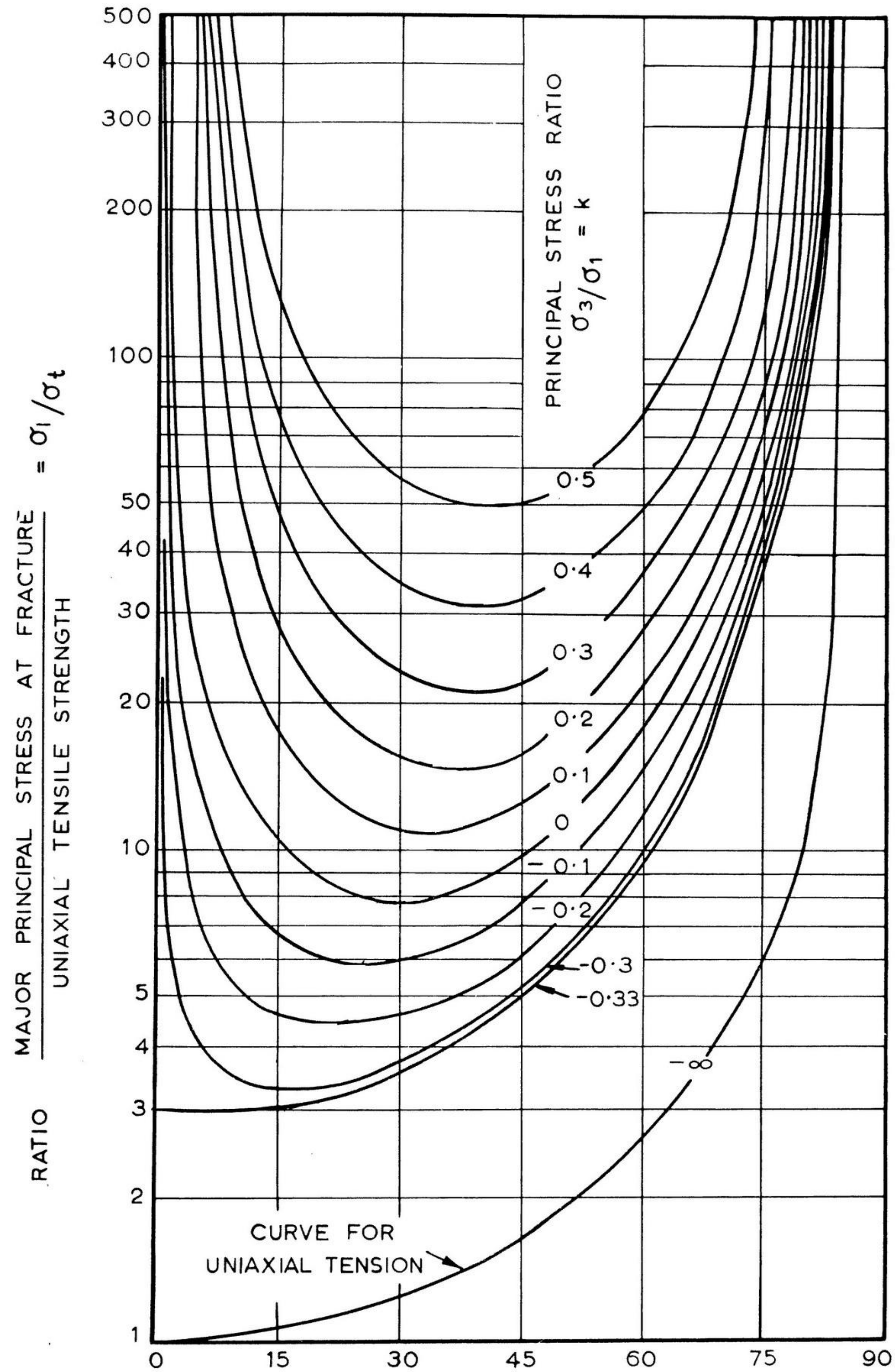

Figure 2. Fracture initiation from a single open Griffith crack inclined at an angle ψ to the major principal stress σ_1.

Differentiating equation (13) with respect to η and equating $\partial\sigma_\eta / \partial\eta$ to zero gives the position on the crack boundary at which the maximum and minimum stresses occur as $\eta = \pm\xi_0$. Substituting these values into equation (13) gives the maximum and minimum tangential stresses on the crack boundary as

$$\sigma_N \cdot \xi_0 = \pm(\tau_{xz} - \mu\sigma_{xx}) \tag{14}$$

Since crack propagation occurs as a result of tensile stress, only the negative value given by this equation need be considered.

Expressing equation (14) in terms of the principal stresses and the uniaxial tensile strength of the material:

$$2\sigma_t = -\frac{1}{2}\{(\sigma_1 - \sigma_3)\sin 2\psi - \mu[(\sigma_1 - \sigma_3) - (\sigma_1 - \sigma_3)\cos 2\psi]\} \tag{15}$$

Differentiating equation (15) with respect to ψ and equating $\partial\sigma_N / \partial\psi$ to zero gives the critical crack orientation at which the highest tensile stresses are induced at the tip of a closed crack as

$$Tan 2\psi_c = {}^{1}\!/_{\mu} \tag{16}$$

Substituting this critical crack orientation into equation (15) gives the fracture criterion for a material in which the highest tensile stresses are induced at the tip of a closed crack as

$$\sigma_1 = \frac{-4\sigma_t}{\left((1-k)\sqrt{1+\mu^2} - \mu(1+k)\right)} \tag{17}$$

Where k is the principal stress ratio σ_3/σ_1.

As in the case of the original Griffith criterion, it is generally assumed that the specimen contains a sufficient number of randomly oriented cracks for fracture to initiate from those cracks which are inclined at an angle defined by equation (16). If, however, the cracks are oriented preferentially as in the case of a highly antistrophic material, it is necessary to consider the inclination of the cracks with respect to the applied stress system. In this case the case the conditions for fracture are determined from equation (15).

In using the modified criterion outlined above, it must be remembered that equations (15) and (17) apply only when the normal stress σ_{xx} is compressive. When σ_{xx} is tensile the original Griffith theory must be applied. A detailed discussion on the transition from the original to the modified fracture criteria has been given by the author in a previous paper[6].

Mohr envelopes for original and modified Griffith Theories

Murrell[10] has shown that the original Griffith theory can be represented by a Mohr fracture envelope which is defined by the following equation:

$$\tau^2 = 4\sigma_t(\sigma_t - \sigma) \tag{18}$$

Brace[11] has shown that the fracture criterion, modified to account for the effects of crack closure in compression, can be represented by a limiting Mohr envelope which is a straight line having the equation

$$\tau = \mu\sigma - 2\sigma_t \tag{19}$$

Fracture criterion for anisotropic rock

Brace[12] has presented evidence which indicates that the cracks, from which the fracture of rock propagates, probably lie within the grain boundaries of the material. Even in rocks of sedimentary origin which exhibit marked foliation and planar anisotropy, the constituent lamellae are made up of grains which are cemented together and hence randomly oriented grain boundary cracks are likely to be present.

In the case of an anisotropic rock, two distinct systems of inherent cracks can be visualized:

a) A set of relatively large preferentially oriented cracks which lie along bedding planes and which may sometimes be in the form of mica flakes;
b) A randomly oriented matrix of grain boundary cracks which are probably several times smaller than the bedding plane cracks.

In the following analysis, the preferentially oriented bedding plane cracks will be referred to as the *primary* crack system while the grain boundary cracks will be termed *secondary* cracks.

In deciding upon the stress required to cause fracture of a particular specimen, it is necessary to consider the inclination of the primary cracks to the applied stress system and to determine whether the tensile stresses induced at the tips of these primary cracks are higher than those which occur at the tips of the most favourably oriented secondary cracks. If the primary cracks are oriented at an angle approaching the critical angle ψ_c, defined by equation (7) or (16), then fracture will generally initiate at the tips of these cracks. If, on the other hand, the primary cracks are parallel or perpendicular to the direction of the major principal stress σ_1, then the tensile stresses induced at the tips of these cracks will be relatively low and very high applied stresses will be necessary to initiate fracture from these cracks (see Figure 2). In this case, fracture will initiate at the tips of the most favourably oriented secondary cracks.

Obviously, the transition from fracture initiation from primary cracks to the propagation of secondary cracks depends upon the physical characteristics of the material, particularly upon the relative crack lengths (ξ_0) and upon whether either or both of the crack systems close under compressive stress (μ). These details are best illustrated by means of a practical example.

A study of the fracture of a South African slate

In order to illustrate the application of the theoretical considerations proposed in this paper and to check their validity, a series of strength determination was carried out on a sample of slate obtained from the Pretoria area. These tests included uniaxial tensile tests parallel to and perpendicular to the bedding planes as well as triaxial compression tests on samples in which the bedding plane orientation was varied, in steps of 15º, from $\psi = 0^{\circ}$ to $\psi = 90^{\circ}$.

Details of the test procedures used by the National mechanical Engineering Research institute for determining the strength of rock materials have not been published previously and a brief description of these techniques is included as an appendix to this paper.

Results of the tests on the slate material are given in Table I. Note that, wherever possible, two specimens were tested for each applied stress condition.

The uniaxial tensile strength of the material perpendicular to the bedding planes can be assumed to be predominantly influenced by the primary crack system (bedding plane cracks). Consequently, this value of tensile strength is denoted by σ_{tp}. The tensile strength parallel to the bedding planes will not be influenced by the primary cracks and fracture can be assumed to initiate at secondary cracks, hence this value of tensile strength is denoted by σ_{ts}.

In order that the results of these tests may readily be compared with the theoretical predications (see Figure 2 for example), the strength values are reduced to dimensionless form by dividing each by the uniaxial tensile strength perpendicular to bedding planes σ_{tp}.

Table 1. Fracture data for a South African slate

1. Uniaxial tensile tests
   a) Tensile strength perpendicular to bedding planes ($\psi = 0°$), $\sigma_{tp} = 660$ and 570 lb/sq.in., average 615 lb/sq.in.
   b) Tensile strength parallel to bedding planes ($\psi = 90°$), σ_{ts} = 2,780 and 3,000 lb/sq.in., average 2,880 lb/sq.in.

2) Triaxial compression tests

$k = \sigma_3/\sigma_1$	k = 0 (uniaxial)		k = 0.113		k = 0.171	
ψ	σ_1 lb/sq.in.	σ_1/σ_{tp}	σ_1 lb/sq.in.	σ_1/σ_{tp}	σ_1 lb/sq.in.	σ_1/σ_{tp}
0	17,600 21,600	28.6 35.2	39,200 36,000	63.7 59.5	55,700 49,300	90.8 80.0
15	6,900 8,700	11.2 14.2	18,300 30,000	29.8 48.0	34,200 39,000	55.6 63.4
30	4,500 4,150	7.3 6.8	7,300 --	11.8 --	8,730 7,840	14.2 12.8
45	5,540 6,560	9.0 10.7	13,900 11,000	22.6 17.9	15,000 16,300	24.4 26.7
60	11,850 11,600	19.3 18.8	24,600 19,400	40.0 31.6	29,600 32,400	48.2 52.6
75	16,000 16,600	26.0 27.0	31,200 31,900	50.7 52.0	41,400 42,900	67,2 69.7
90	15,600 16,100	25.3 26.2	30,600 --	49.8 --	41,700 39,300	68.0 64.0

From the results presented in Table 1, the behaviour of the primary and secondary crack systems of the slate can be approximated.

In the case of the primary cracks, the compressive fracture behaviour of the specimen will be most strongly influenced by these cracks when they are oriented at between 30° and 35° if the cracks remain open (equation (7)). If the cracks close under compression, they will exert their strongest influence when inclined at an angle defined by equation (16).

Examination of the experimental results reveals that the compressive strength of the slate is lowest when the bedding planes are inclined at approximately 30° to the direction of the major principal stress. Consequently, it can be concluded that the cracks have either remained open or that, if they have closed, the coefficient of internal friction μ has a value of approximately 0.6.

In an attempt to establish which of these two possibilities is most likely, a Mohr fracture diagram for the primary crack system was plotted and is illustrated in Figure 3. In plotting the Mohr circles, the tensile strength used is that obtained fro tests perpendicular to the bedding planes. The Mohr circles for uniaxial and triaxial compressive values are taken as those given for tests in which the bedding planes were inclined at 30º to the direction of the major principal stress.

On the basis of the limited number of test results available, the indications are that the primary cracks have remained open and that the original Griffith fracture criterion can be applied to them. However, caution must be exercised in drawing definite conclusions from so few results and, in the following analysis, both possibilities outlined above will be explored.

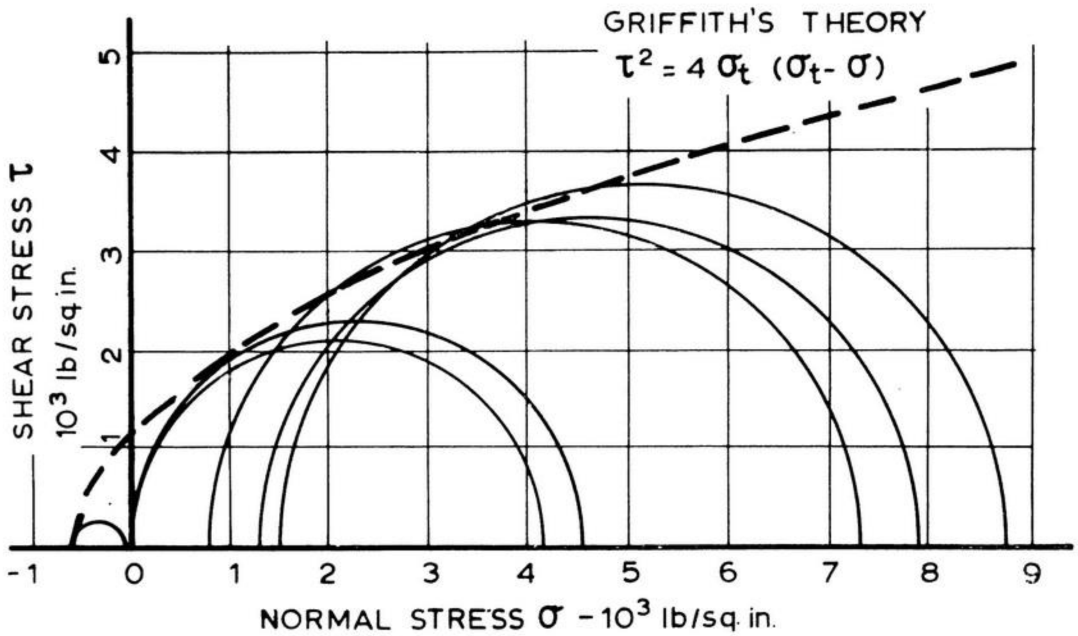

Figure 3. Mohr fracture diagram for primary crack system of slate

Behaviour of the secondary crack system is fairly clearly defined by the Mohr fracture diagram presented in Figure 4. In this case, it can be anticipated that the cracks will be initially closed and it will be seen that the modified Griffith fracture criterion offers a reasonably good prediction of the observed behaviour. In plotting the Mohr diagram illustrated in Figure 4, the tensile strength parallel to the bedding planes (σ_{ts}) has been used. Compressive fracture data for specimens tested at $\psi = 0^{\circ}$ and $\psi = 90^{\circ}$ are included since these values should not be influenced by the primary cracks.

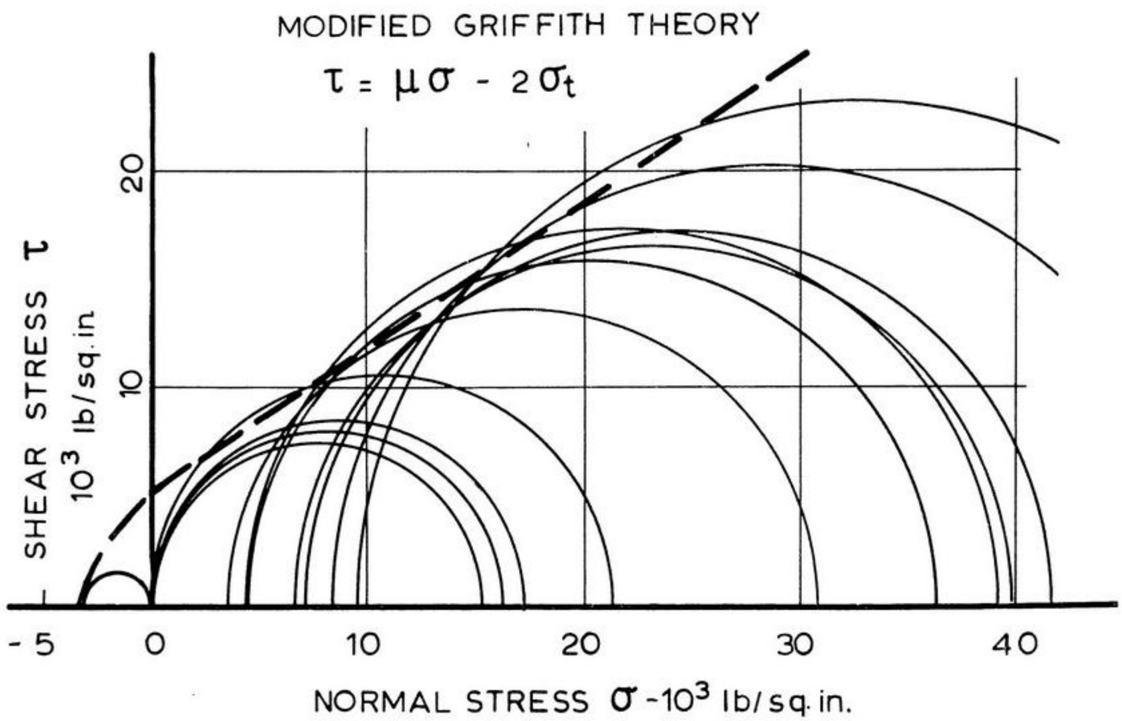

Figure 4. Mohr fracture diagram for secondary crack system of slate

The influence of the bedding plane orientation upon the uniaxial compressive strength and upon the strength of the slate, when subjected to triaxial stress conditions in which the principal stress ratio k = 0.171, is illustrated in Figures 5 and 6. In these graphs, the experimental results are compared with the behaviour predicted by both the original Griffith theory and by the modified fracture criterion.

The dipping portions of the theoretical curves are obtained by solving equation (10) for the original Griffith theory and equation (15) for the modified fracture theory. In both cases σ_t is taken as σ_{tp} = 615 lb/sq.in. The value of the coefficient of internal friction μ substituted into equation (15) is 0.6 as deduced above.

The straight line portions of the theoretical curves are obtained from equation (17), substituting $\sigma_t = \sigma_{ts} = 4.7\sigma_{tp}$. The coefficient of internal friction used in this case was determined form the slope of the Mohr envelope presented in Figure 4 and was found to be 0.61.

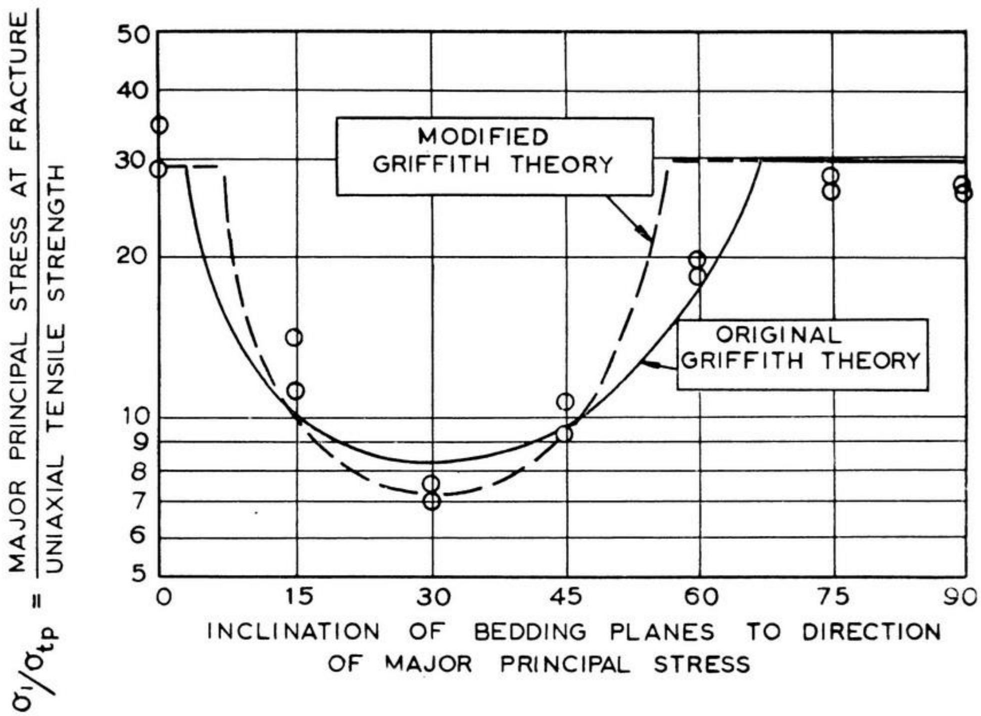

Figure 5. Influence of bedding plane orientation on the uniaxial compressive strength of South African slate

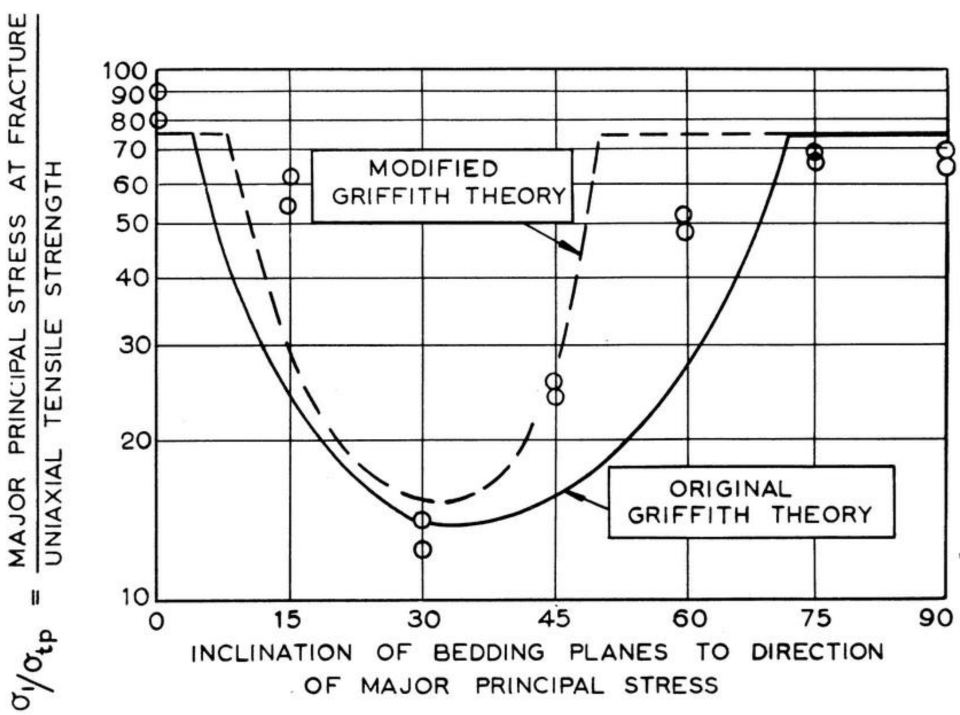

Figure 6. Influence of bedding plane orientation on triaxial compressive strength (K = 0.171) of South African slate

Discussion of results

The primary purpose of attempting to formulate a theoretical fracture criterion such as that outlined in this paper is to facilitate the interpretation and rationalisation of experimental results. Unless such a fundamental theory exists, the results presented in Table 1 are merely an interesting example of material behaviour which applies to this particular sample of slate only. If, however, the experimental results can be compared with and are found to substantiate the theoretical predictions, then they become part of a rational behaviour pattern which can be extended to cover other materials.

Note that equations (10), (15) and (17), which have been used to predict the theoretical fracture behaviour of this sample of slate, depend only upon two material constants, namely the uniaxial tensile strength and the coefficient of internal friction. If these equations are found to be generally applicable to materials of this type, a reliable prediction of their fracture behaviour could be made on the basis of a few simple physical tests.

In spite of the approximations which have been made in deriving this theory the agreement between the predicted and observed facture behaviour of slate is encouraging. Results of similar tests on Martinsburg slate from Pennsylvania in the United States of America have been presented by Donath [1, 2]. Although the results have been presented in a form which makes a complete analysis difficult, a number of approximate checks have indicated that Donath's results would also be in good agreement with the theory.

Considering the present empirical nature of the science of rock mechanics, the accuracy of prediction offered by these theoretical considerations is adequate for most practical purposes. It is believed that more detailed experiments as well as more sophisticated mathematical treatment could be used to refine the existing theory, if and when an improvement in accuracy becomes necessary.

Although the present theory is based upon the assumption that only two distinct crack systems are present in an anisotropic material, it is obvious that these arguments can be extended to the case where two or more major crack systems are superimposed upon the randomly distributed grain boundary cracks. Such an extension would probably prove useful in the analysis of fracture of coal where cleats as well as bedding planes are present.

An important conclusion which can be drawn from the results presented in this paper is that compression tests parallel to and perpendicular to the bedding planes are not sufficient to define the fracture behaviour of an anisotropic material. There is a tendency to conclude that a material is isotropic with respect to strength if its compressive strength perpendicular and parallel to the bedding planes is the same. Examination of Figures 5 and 6 reveals that this deduction can be grossly in error.

The simplest test for strength isotropy is to compare the uniaxial tensile strength parallel to and perpendicular to the bedding planes. Failing this, a compression test in which the bedding planes are included at approximately 30º to the major principal stress direction should be included in the test programme.

The author wishes to avail himself of this opportunity to emphasize the importance of choosing the correct specimen geometry and test conditions for strength determination of rock materials. If the calculated stress at fracture requires anything more than a simple division of applied load by cross-sectional area, the results of strength tests will probably be unreliable. This is particularly true of an anisotropic material where not only the strength but also the stress distribution in the specimen are markedly influenced by anisotropy.

As an example of an uncertainty involved in indirect strength tests, the case of the uniaxial tensile strength of the specimen of slate discussed in this paper is quoted.

Direct tensile tests on carefully designed and prepared specimens (see Appendix) gave the tensile strength perpendicular to the bedding planes as 615 lb/sq.in. and that parallel to the bedding planes as 2,880 lb/sq.in..

Indirect tests in which a tensile stress is induced in the centre of a disc subjected to diametral compression[3] gave values of 438 lb/sq.in. perpendicular to the bedding planes and 1,310 lb/sq.in. in parallel to the bedding planes.

Correct specimen design is equally important for compression specimens and the same laws apply whether the specimen being tested is a single rock grain or a block of rock of 10 ft cube. Only if the stress conditions in the specimen are accurately known can the results be interpreted with any degree of certainty.

Conclusions

It has been shown that Griffith's theory of brittle fracture, modified where necessary to account for the effects of crack closure in compression, can be used to predict the fracture behaviour of a material such as slate which exhibits a high degree of planar anisotropy.

It is suggested that this theory could be extended to the case of a material such as coal which may have several major weakness planes oriented at various angles to each other.

While the accuracy of the present theory is regarded as adequate for most practical purposes, it is believed that, if necessary, refinements to this theory are possible.

As a result of this study, it is concluded that special care should be exercised in planning strength tests on anisotropic material. It is particularly important that deductions should not be made unless adequate experimental data is available.

Acknowledgements

The author wishes to express his appreciation to the owners of the Elliot Slate Quarries in Pretoria for supplying the sample of slate used in these tests, to Mr. J.B. Kennard for his careful preparation of the specimens and to Mr. U.W.O.L. Vogler and Mr. H.K. van der Merwe for carrying out the tests.

The permission of the South African Council for Scientific and Industrial Research to publish the material contained in this paper is acknowledged.

Appendix – Equipment and experimental techniques used for the determination of strength of rock materials

Experimental verification of the theoretical postulates contained in this and in a previous paper[6], necessitates the loading of specimens of rock to fracture under various accurately known and controlled stress conditions. This appendix contains a brief description of the triaxial test apparatus, designed by the author and used by the Rock Mechanics division of the National Mechanical Engineering Research Institute for compressive tests on rock material. Details of the specimens used for the determination of tensile strength are also given.

Triaxial test apparatus

The triaxial test apparatus, illustrated diagrammatically in Figure 7, is designed to apply a constant ratio of lateral hydraulic pressure to axial stress in the specimen. This is achieved by loading the specimen in series with a piston and cylinder unit which generates the hydraulic pressure.

If the diameters of the loading piston, specimen and pressure piston are denoted by D_L, D_S and D_p respectively, then the lateral stress σ_3, which is equal to the hydraulic pressure acting on the specimen, is given by

$$\sigma_3 = \frac{4L}{\pi D_p^2} \tag{1A}$$

Where L is the total load applied to the loading and pressure pistons.

The axial stress σ_1 in the specimen is given by the following equation

$$\sigma_1 = \frac{4L}{\pi D_S^2}\left\{1 - \frac{D_L^2 - D_S^2}{D_p^2}\right\} \tag{2A}$$

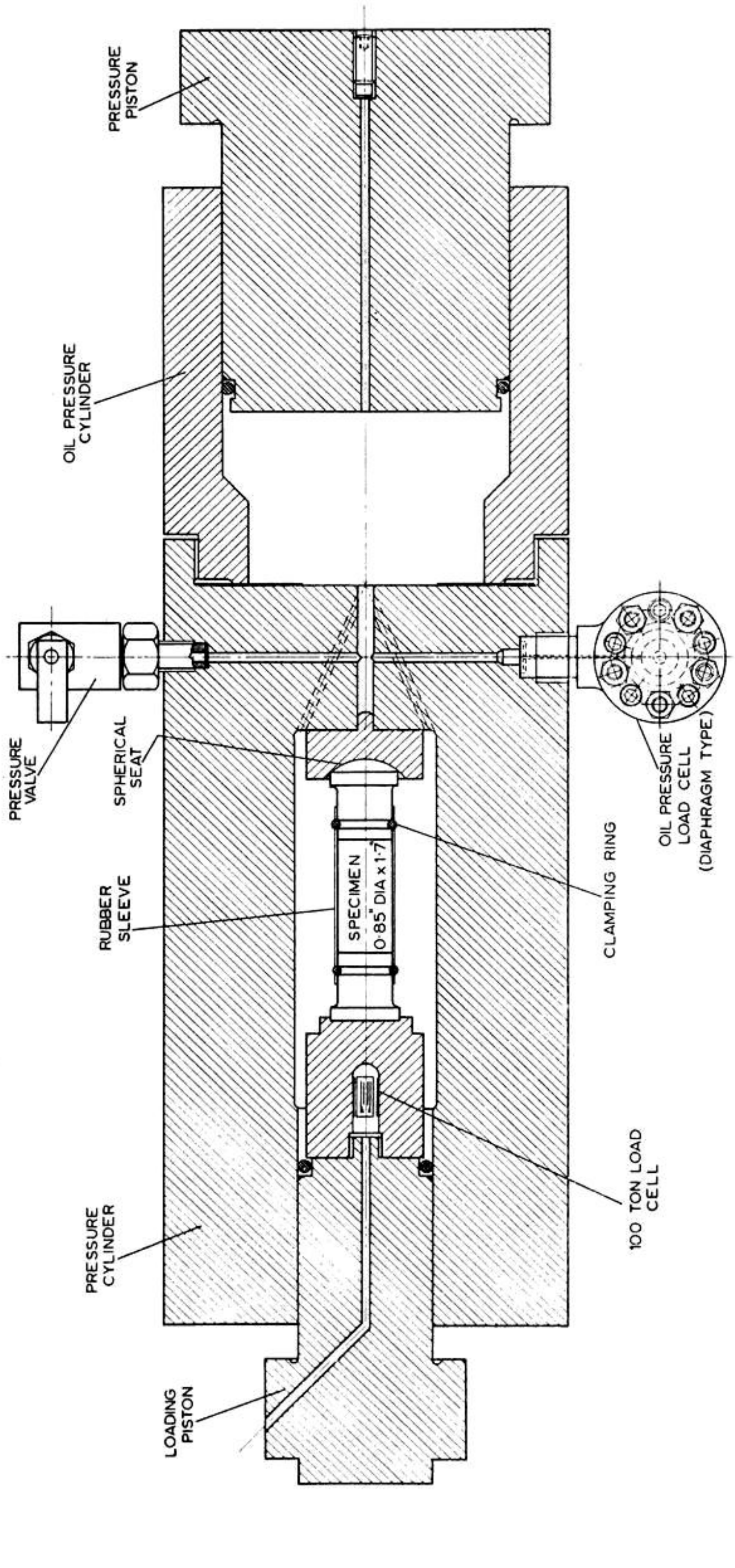

Figure 7. Triaxial test apparatus

The apparatus, illustrated in Figure 7, for testing EX core specimens (0.85 in. diameter) has been designed for applying axial stresses (σ_1) of up to 350,000 lb/in.^{2} and lateral stresses (σ_3) of up to 35,000 lb/in.^{2} . The ratio of σ_3/σ_1, which is chosen for any particular test depends upon the diameter of the pressure piston D_p which is used.

Changes in the stress ratio σ_3/σ_1 are achieved by replacing the entire oil pressure cylinder and piston unit with another of a different diameter. Sealing between the oil pressure cylinder and the body of the test cell is achieved by a method which was originally suggested to the author by Professor G.T. van Rooyen at Pretoria University. The principal features of this method are illustrated in Figure 8.

The oil pressure cylinder is attached to the test cell body by means of a loosely fitting thread – designed to provide location and initial sealing only. A thin deformable gasket of the impregnated paper type is placed between the sealing faces and serves to compensate for any irregularities of these faces and to provide initial sealing.

Once the oil pressure is generated by the application of load, the thread load is relieved and the gasket is acted upon by a force which is directly proportional to the oil pressure. Since the area A of the sealing face is smaller than the area B of the step in the cylinder wall, the sealing pressure on the gasket is always greater than the pressure of the oil trying to escape and hence the device is self-sealing.

The moving seals on the loading and pressure pistons are a combination of neoprene rubber 'O'–rings and brass anti-extrusion rings as illustrated in Figure 9. At the high pressures dealt with in this application, extrusion of the rubber rings into the clearance gap between piston and cylinder becomes a serious problem unless special steps are taken to prevent it. The provision of an anti-extrusion ring of the type illustrated ensures that there is virtual metal to metal contact between this ring and the cylinder wall and extrusion of the rubber is thereby prevented. The anti-extrusion ring is made from a softer metal than the cylinder to prevent scoring of the ground cylinder wall.

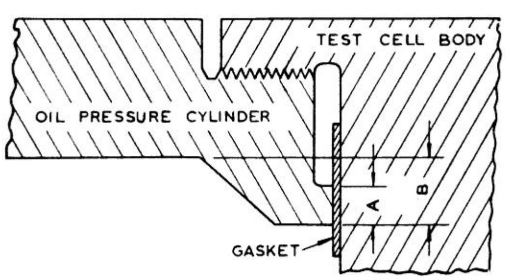

Figure 8. Detail of self-sealing joint between oil pressure and test cell body.

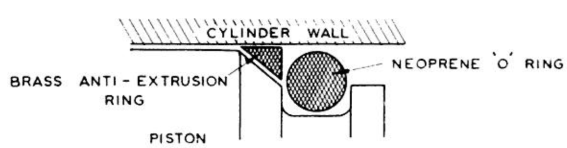

Figure 9. Detail of high pressure moving seal.

These sealing devices have proved to be completely reliable for the range of pressures generated in this apparatus. Measurements have shown that the frictional resistance due to the moving seals is very low – of the order of 1 per cent of the hydraulic pressure.

Although the neoprene rings and anti-extrusion rings are regarded as expendable items and can easily be replaced, it has not been found necessary to replace the original sealing units in spite of the fact that several hundred triaxial tests have already been completed.

The specimens used for the triaxial tests described in this paper consist of 1.7 in. length of standard EX diamond drill core (0.85 in. diameter). The ends of the specimen are ground flat and parallel but no additional grinding of the cylindrical surface is necessary. The specimen is loaded between hardened steel platens as illustrated in Figure 7. A spherical seat at the base of one of these platens eliminates bending in the specimen.

The specimen is sheathed in a thin rubber sleeve as illustrated and this effectively prevents ingress of the pressurized hydraulic fluid.

The load applied to the specimen is measured by means of a strain gauge type load cell which is loaded in series with the specimen. Provision is also made of measurement of the hydraulic pressure. The deformation of the specimen is measured by means of a linear potentiometer which measures the displacement between the loading piston and the test cell body.

During a test, the electrical outputs of the load cell (or pressure gauge) and the linear potentiometer are plotted automatically on an X-Y recorder. The resulting load-deformation graph is then converted to a stress-strain graph by applying experimentally determined calibration factors.

The triaxial test apparatus together with its loading frame and the X-Y recorder are shown in the photograph which is reproduced in Figure 10.

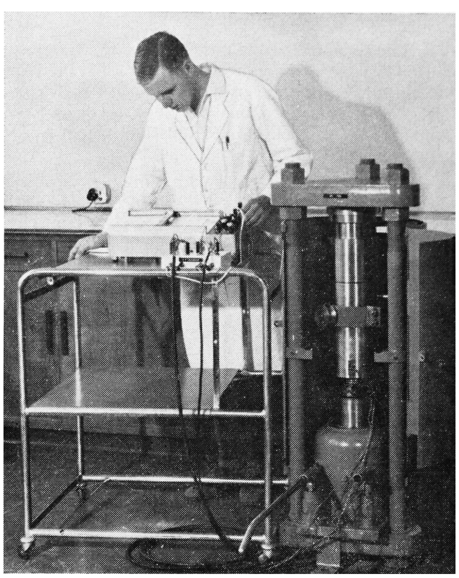

Figure 10. Triaxial compression test apparatus set up in a 100 ton loading frame.

Tensile test specimens

Tensile testing of rock materials is generally regarded as difficult because of the problem of gripping the specimen. After a great deal of unsuccessful effort had been devoted to devising methods for gripping specimens, the author came to the conclusion that, if the results of tensile tests are to have any meaning, correctly shaped tensile specimen are essential.

The shape of the tensile specimen which is used by the Rock Mechanics Division of the national mechanical Engineering Research institute is illustrated in Figure 11.

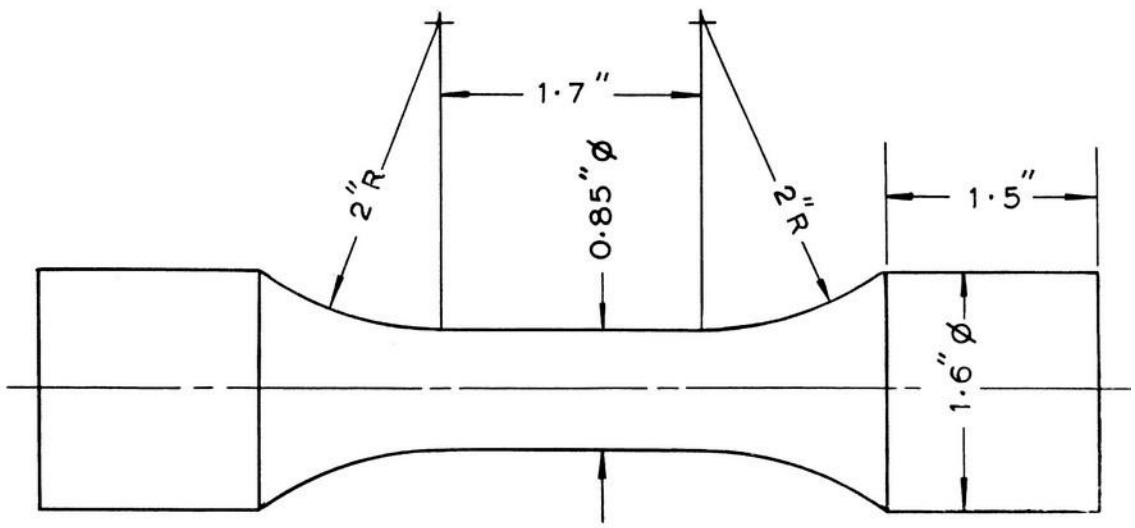

Figure 11. Detail of tensile specimen

Note that the actual 'test section' is 0.85 in. diameter by 1.7 in. long, in other words, it has the same dimensions as the compression specimen. The fillets forming the transition between the test section and the gripping section are designed to reduce the stress concentration at this transition to a minimum. The specimen is gripped by means of conventional wedge type grips and the tests which have been carried out on such specimens are regarded as completely successful.

The specimens are prepared by grinding with a high speed water-cooled diamond wheel. The grinding attachment is carried on the tool post of a lathe and the profile of the specimen is generated by a profile and follower device which is actuated by the lead screw of the lathe. This grinding attachment, illustrated in Figure 12, was designed by Mr. J. B. Kennard of the rock Mechanics Division of the National Mechanical Engineering Research Institute.

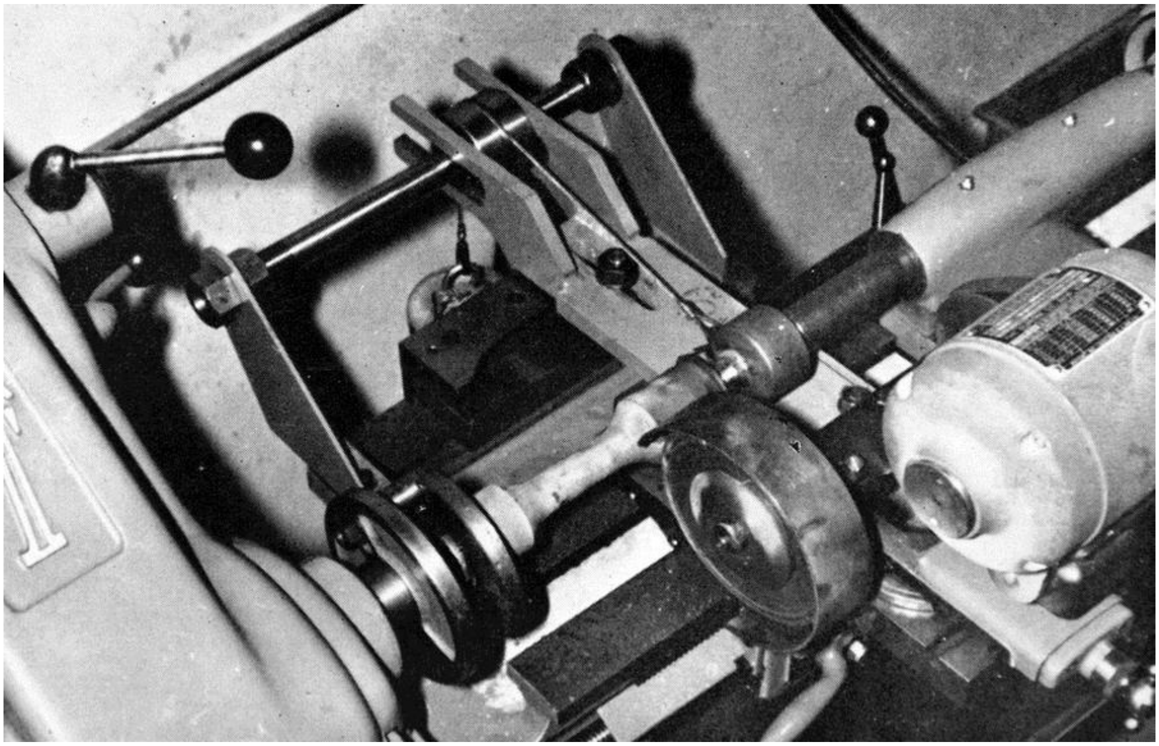

Figure 12. Grinding attachment for the preparation of tensile specimens of rock materials

References

1. Donath, F.A. (1961). "Experimental study of shear failure in anisotropic rocks." *Geophysical Society of America Bulletin*. Vol. 72, June, pp. 985-990.

2. Donath, F.A. (1963). "Strength variation and deformation behaviour of anisotropic rock." Preprints of papers. International Conference on the State of Stress in the Earth's crust, Santa Monica, June 1963. *The Rand Corporation Memorandum* RM-3583, pp. 5/1-9.

3. Berenbaum, R. and Brodie, I. (1958). Measurement of the tensile strength of coal: A critical assessment and the application of a new technique." *National Coal Board Scientific Department, Mining Research Establishment*, Report No. 2109, 1958.

4. Griffith, A.A. (1921). "The phenomena of rupture and flow in solids." *Philosophical Transactions of the Royal Society, London, A*. Vol. 221, pp. 163-197.

5. Griffith, A.A. (1924). "Theory of rupture." *Proceedings of the First International Congress for Applied Mechanics*, Delft,. J. Waltman Jr., 1255, pp. 55-63.

6. Hoek, E. (1963). "Rock fracture around mine excavations.: CSIR Rock Mechanics Special Report No. 38". To be presented to International Conference on Strata control and Rock Mechanics, New York, 1964.

7. Orowan, E. (1949). "Fracture and strength of solids." *Reports on Progress in Physics,* Vol. 12. The Physical Society, pp. 182-232..

8. Inglis, C.E. (1913). "Stresses in a plate due to the presence of cracks and sharp corners." *Institution of Naval Architects,* London, pp. 219-230.

9. McClintock, F.A. and Walsh, J.B. (1962). "Friction on Griffith cracks in rocks under pressure." *International Congress on Applied Mechanics,* Berkeley, in Press.

10. Murrell, S.A.F. (1958). "The strength of coal under triaxial compression." *Mechanical properties of non-metallic Brittle Materials, Butterworth Scientifc Publications,* pp. 123-145.

11. Brace, W.F. (1960). "An extension of Griffith theory of fracture to rocks." *Journal of Geophysical Research*, Vol. 65, No. 10, pp. 3477-3480.

12. Brace, W.F. (1961). "Dependence of fracture strength of rocks on grain size." *Bulletin of Mineral Industries Experimental Station*. Penn. State University, No. 76, pp.99-103.